Smart Structures and Systems, *Vol. 27, No. 3 (2021) 457-466*
DOI: https://doi.org/10.12989/sss.2021.27.3.457

A multi-time scale vibration surveillance system for third-party threats on urban pipeline

Zelong Liu [1], Renzhu Peng [1], Yan Zhang [1] and Suzhen Li*[1,2]

[1] *College of Civil Engineering, Tongji Univeristy, Siping 1239, Shanghai, China*
[2] *State Key Laboratory of Disaster Reduction in Civil Engineering, Tongji Univeristy, Siping 1239, Shanghai, China*

(*Received November 7, 2019, Revised November 16, 2020, Accepted December 29, 2020*)

Abstract. Third-party interference caused by construction activities have seriously jeopardized the security of underground pipelines. Following the process of "signal collection—feature extraction and selection—multi-time scale identifying—combining results by voting", this paper proposes a multi-time scale surveillance system for interference prevention of third-party threats on the nearby pipeline by using ground vibration monitors. The system focuses on the two major urban construction activities induced by excavator breaking hammers and road cutters, and presents excellent performance under the noise of traffic and pedestrian. Three features including the short-time zero-crossing rate, subset differential parameter and the Mel frequency cepstrum coefficients are selected by the analysis of the maximal information coefficient and feature importance for identifying the patterns of different third-party activities. The crucial part of the surveillance system consists of the two random forest-based classifiers trained by 0.5 s samples and 8 s samples respectively, and the alarm depends on the voting of the two classifiers, which brings the perspectives on different time scales for decision making. In the test, 96.14% of the threat vibration signals can be detected, while only 0.45% of the environmental noise signals cause false alarms.

Keywords: underground pipeline; third-party interference; multi-time scale; ground vibration monitoring; vibration signal feature; feature selection; random forest

1. Introduction

In modern society, urban pipelines play an important role for matter and energy transmission. The third-party interference that mainly refers to civil construction, human intrusion and other interference account for 29.8% and 28% of all pipeline accidents in the United States (PHMSA 2017) and Europe (EGIG 2018), and this percentage even reaches 68% in China because of the frequent civil construction (Zhang and Li 2018). Such a serious situation requires an effective real-time surveillance system to protect urban pipelines from the third-party threats.

The passive measures are currently the most common methods of preventing the third-party interference, including placing warning boards and caution tapes or setting up one-call systems (Muhlbauer 2004). However, these passive measures highly depend on the support from constructors and lack effective restrictions on malicious behavior. To enhance the ability of active supervision, more techniques have been recently developed for real-time monitoring of pipelines subjected to external intrusions. Using the sound signals from microphones, Wan *et al*. design and test a system to recognize acoustic records of the road cutter based on support vector machine (SVM) (Wan and Mita 2009). Another study of acoustic monitoring system is that of Jiang (Jiang *et al*. 2018), in which sound signals collected by fiber distributed acoustic sensing (FDAS) systems along pipelines are used for identifying third-party interference. The video/image monitoring system is widely applied in protecting city gate stations and other important infrastructures by the fixed cameras (Banu *et al*. 2017, Fernández *et al*. 2013, Zhang *et al*. 2015, Zhu *et al*. 2019). It can also be applied for prevention of third-party interference based on the image recognition results of aero-photograph (Hausamann *et al*. 2005, Liu *et al*. 2014, Li *et al*. 2019), but the aircraft inspection is generally limited by weather condition and high buildings in the city. Vibration signals caused by the third-party interference can be recorded by optical fiber (Peng *et al*. 2014, Tejedor *et al*. 2017, Sun *et al*. 2015, Tejedor *et al*. 2018, Wang *et al*. 2019, Wu *et al*. 2015), static sensing cable or multiple acceleration sensors (Sun and Wen 2013), which shows the superior ability of detecting and locating third-party activities. However, it is essential to excavate ground in the installation of the optical fiber and the sensing cable, which usually causes city traffic jams and expensive costs. By contrast, the employment of the multiple acceleration sensors has attracted attention recently for the convenience of layout.

Due to the similarity of monitoring signals for ground vibration, the third-party interference surveillance system has a lot in common with the earthquake monitoring system. Actually, the earthquake monitoring systems have been set up for some important lifeline infrastructures, for example, gas facilities, to make earthquake emergency

*Corresponding author, Associate Professor,
E-mail: Lszh@tongji.edu.cn

ISSN: 1738-1584 (Print), 1738-1991 (Online)

responses (Ghatak *et al*. 2014, Makhoul *et al*. 2018). The wireless sensor network developed for earthquake monitoring is an excellent signal collection method that can also be applied to monitor the ground vibration due to third-party activities (Bock *et al*. 2011, 2004, Fahmy 2016, Okada *et al*. 2004). However, more efforts are required for vibration signal recognition, because the types of the third-party interference are diverse and the complicated urban environmental noise may make the recognition rate worse. The improvement of feature extraction methods and classification algorithms is desired for this specific application scenario.

Based on ground vibration monitoring, this paper proposes a multi-time scale surveillance system for intrusion prevention of third-party threats on urban pipelines. The rest of this paper is arranged as follows: Section 2 presents the dataset acquired from field tests, in which the vibration signals of construction equipment and environmental noise are compared in time and frequency domain. Section 3 presents the subset differential parameter feature and the Mel frequency cepstral coefficient feature reconstructed by the principal component analysis. The two features are then compared with common vibration signal fatures by the analysis of the maximal information coefficient and the feature importance for feature selection. In the section 4, the different time scale classifiers are trained and combined for the best multi-time scale classifier combination. Section 5 proposes a voting strategy to combine the results from the two classifiers of section 4 and validates the proposed monitoring system. Finally, the conclusions are drawn in section 6.

Table 1 Vibration record

Third-party interference	Distance between sensor and equipment (m)	Duration (s)	
		Traffic noise	Pedestrian noise
Road cutter	3*, 5, 10*,15,20*	1230	1130
Excavator breaking hammer	5, 10*, 15, 20*, 25, 30*, 35, 40, 45	350	350
No construction equipment	N/A	670	87440

*The sensors of the ranges with asterisks are placed on the manhole cover

2. Field tests for ground vibration signals

2.1 Field tests

Most urban pipelines are buried under the roads for the convenience of in-situ placement and medium transportation. The third-party threats on the pipeline are mainly posed by the road works exerted by excavator breaking hammers and road cutters. In the field tests, the vibration signals induced by the two construction activities are collected, as well as pedestrian noise and traffic noise representing the typical urban environmental noise. As presented in Figs. 1(a)-(d), the signals are acquired by piezoelectric accelerometers which are placed on the road surface and the manhole cover to investigate the effect of the site condition on the vibration signal transmission. An over 25-hour database with a sampling rate of 2 kHz is ultimately established to support the further research of surveillance system, and the record details are given in Table 1.

2.2 Preliminary comparison of vibration signals

The time series of the threat signals are first compared with the two kinds of noise signals, as plotted in Fig. 2. The amplitudes of the excavator breaking hammer follows a cyclical pattern that distinguishes it from the other collected signals. In terms of amplitude, the road cutter and the two types of the environmental noise are much lower than the breaking hammer. It indicates that the excavator breaking

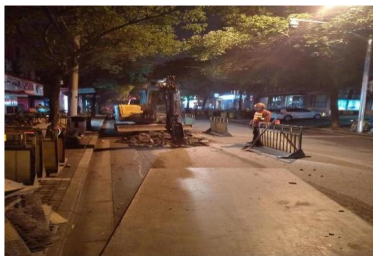

(a) Excavator breaking hammer

(b) Road cutter

(c) The sensor placed on the manhole cover

(d) Traffic noise

Fig. 1 Scenarios for collecting vibration signals

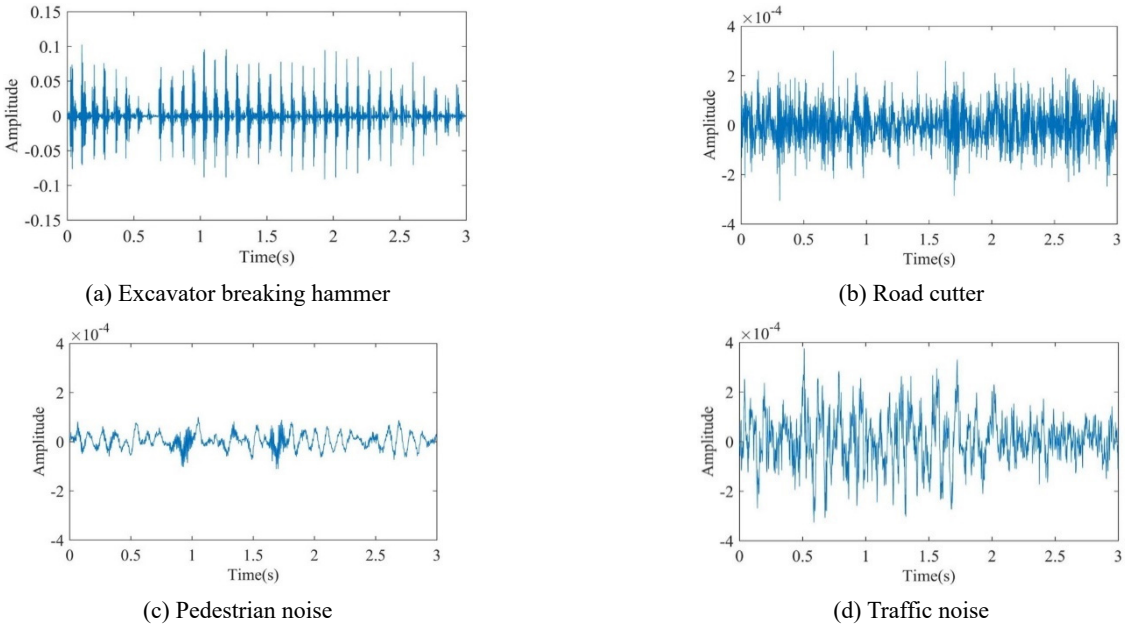

(a) Excavator breaking hammer (b) Road cutter

(c) Pedestrian noise (d) Traffic noise

Fig. 2 Comparison of third-party interference and environmental noise in time domain

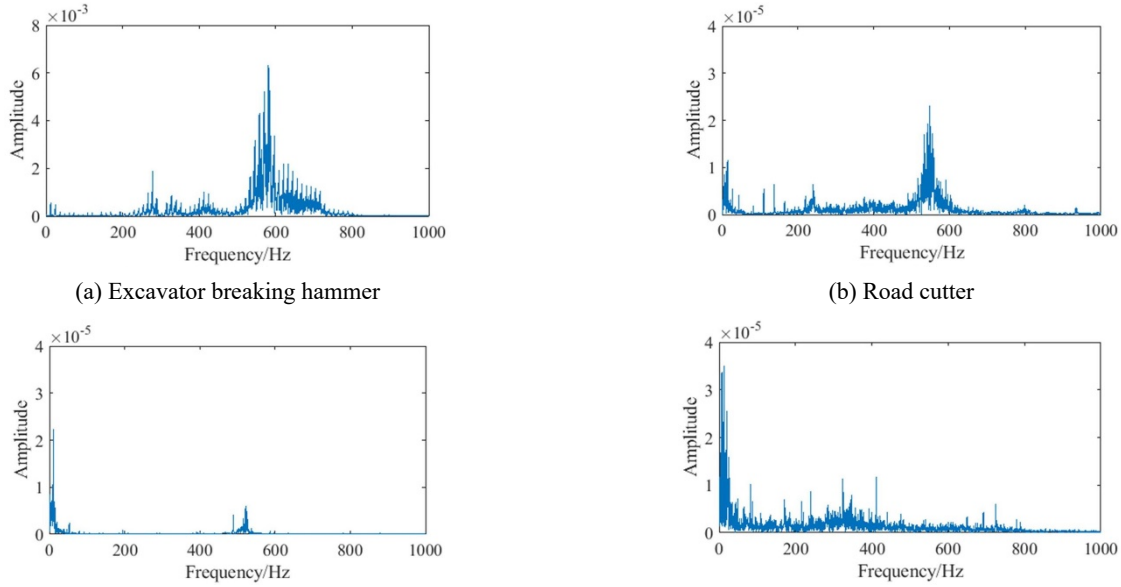

(a) Excavator breaking hammer (b) Road cutter

(c) Pedestrian noise (d) Traffic noise

Fig. 3 Comparison of third-party interference and environmental noise in frequency domain

hammer can be easily distinguished from the pedestrian noise and the traffic noise. However, due to the similarity of the time-series data, it is difficult to separate the road cutter signals and the traffic noise in time domain.

Fig. 3 presents the vibration signals of the third-party interference and the environmental noise in frequency domain. For the excavator breaking hammer, the dominant frequencies concentrate around 580 Hz. There are several multiple peaks in the spectrum of the road cutter, the most obvious one of which is 550 Hz. The high-frequency components in the signals are caused by the short-duration strong impact of the excavator hammer and the road cutter on the ground (Zhang 2018). The main frequencies of the environmental noise are remarkably lower than those of construction vibration. Both the pedestrian noise and the traffic noise have peaks below 50 Hz, and attenuate significantly in the high frequency region. In short, the difference in high frequencies may form a crucial basis to identify the third-party interference under urban environmental noise.

3. Feature extraction and selection

Since the acoustic signals are short-time stationary, it is necessary to separate the records into samples before extracting the features. The specific method is to slide a fixed-size window on the time series and to take the

fragments within the window as samples. A hamming window function is employed to reduce high-frequency signals caused by segmentation. All the samples can be obtained by

$$y_i(n) = Ham(n) \times x[(i-1) \times d + n], \quad 1 \le n \le s \quad (1)$$

where $y_i(n)$ is the n-th value of the i-th sample in time domain, $Ham(n)$ is the hamming window function, x is the record to be divided, d is the distance of each sliding and s is the size of window.

This section proposes a new feature called subset differential parameter to reflect the volatility of vibration signals. The Mel frequency cepstral coefficient (MFCC), which is a classical feature in speech recognition, is calculated and processed by principal component analysis (PCA) to obtain the frequency characteristics of vibration signals (Martínez and Kak 2001, Zheng *et al*. 2001). The two features are then compared with the common features of vibration signal by the analysis of the maximal information coefficient (MIC) (Reshef *et al*. 2011) and the feature importance ranking.

3.1 Subset differential parameter

The subset differential parameter feature is proposed to provide an indication of the volatility between the two consecutive samples. As shown in Fig. 4, the calculation process can be divided into the following five steps:

(1) Dividing the two time adjacent samples into $2 \times w$ subsets (the w is usually set to a constant between 10 and 100);
(2) Calculating the mean value of each subset (V_{1q} and V_{2q});
(3) Obtaining $1 \times w$ difference values ($Diff_q$) by calculating the differences between the corresponding subset mean values of the two samples;
(4) Calculating $1 \times w$ absolute values (Abs_q) of the difference values;
(5) Summing the absolute values to get the subset differential parameter feature.

Figs. 5(a)-(b) present the subset differential parameter features of 0.5 s samples and 8 s samples under the four conditions. Compared with the results obtained by 0.5 s samples, the subset differential parameter features of 8 s samples have better performances in detecting third-party threats.

3.2 MFCC-PCA feature

MFCC is a feature in the frequency domain based on mechanism of human hearing, and the calculation process of MFCC includes the following steps.

(1) Pre-emphasis processing is first required to boost the high-frequency performance of the sample. The sample are processed by a pre-emphasis filter that can be expressed as

$$p(n) = 1 - \alpha[y(n)]^{-1} \quad (2)$$

where $p(n)$ is the sample to be filtered and α is a constant generally set to 0.95.
(2) The time series data are then converted to frequency domain by Fast Fourier Transform (FFT)

$$P(k) = FFT[p(n)] \quad (3)$$

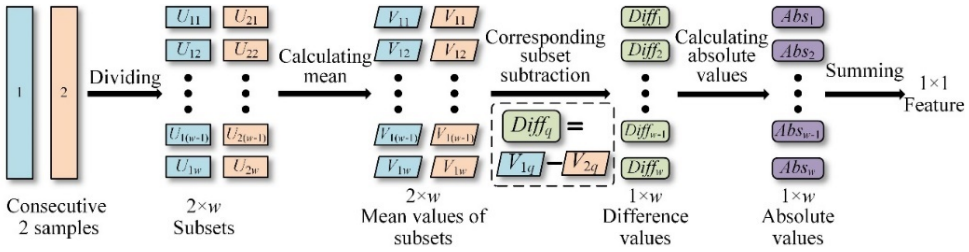

Fig. 4 Calculation process of subset differential parameter

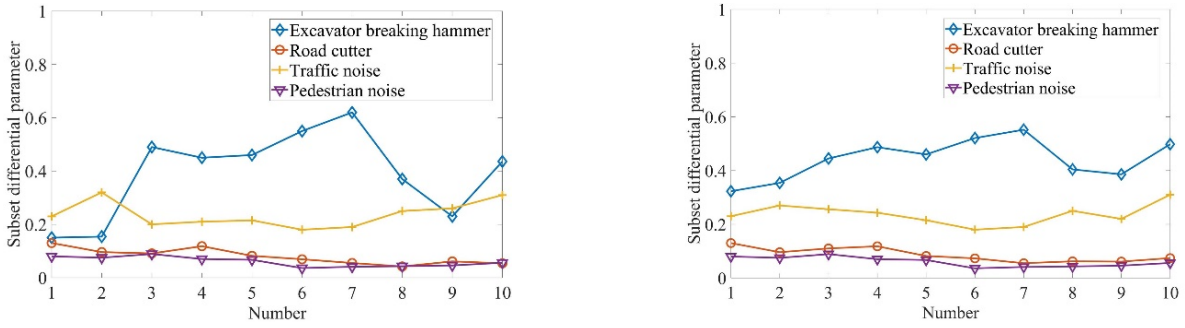

(a) 0.5 s samples (b) 8 s samples

Fig. 5 Subset differential parameter features in different time scales

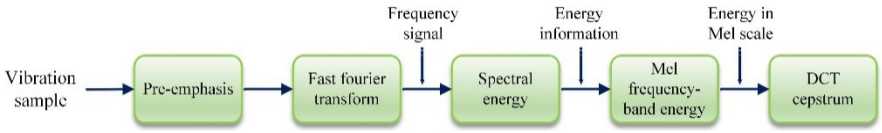

Fig. 6 MFCC calculation procedure

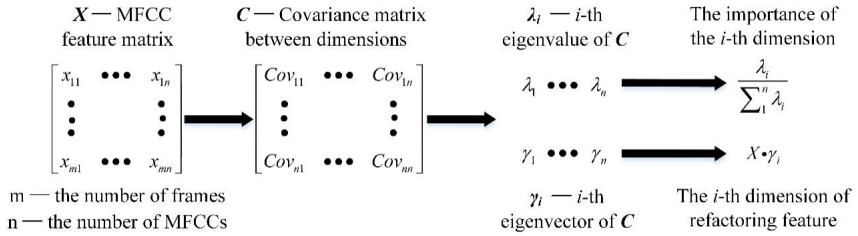

Fig. 7 PCA process

where $P(k)$ is the amplitude at k Hz, and the maximum value z of the frequency k is half of the sampling rate, which is 1000 in this paper.

(3) The spectral energy of the sample can be obtained by

$$E(k) = [P(k)]^2 \tag{4}$$

(4) The energy spectrum in frequency domain is then filtered by the Mel filter bank, and the energy in each Mel filter can be calculated as follows

$$G(e) = \sum_{k=0} E(k) D_e(k), \quad 0 \le e < M \tag{5}$$

where $G(e)$ is the e-th Mel filter energy, $D_e(k)$ is the filter function of the e-th bandpass filter and M is the total number of Mel filters generally taken as 12.

(5) The logarithms of Mel filter energy in Eq. (5) are calculated *and then processed* by the discrete cosine transform (DCT) for MFCC. MFCC can be expressed as

$$MFCC(e) = \sqrt{\frac{2}{M}} \sum_{e=0}^{M} log[G(e)] \cos\left[\frac{\pi h(2e-1)}{2M}\right] \tag{6}$$

where $MFCC(e)$ is the e-th MFCC.

The MFCC feature of every sample has 12 dimensions, which increases the complexity of recognition and reduces the response speed of the monitoring system. Therefore, the PCA method is applied to reconstruct the MFCCs with fewer dimensions while retaining enough information. In this method, the variance of the data is assumed to be positively correlated with the amount of information contained in the data. The main goal of this method is to find the orthogonal coordinate system with the largest sum of variances for each dimension, and the processing flow is presented in Fig. 7. Because the importance ranking in the Fig. 8 indicates the first three dimensions contain 71.2% of the information, the MFCC-PCA feature is finally defined as the first three dimensions of the MFCCs reconstructed by PCA.

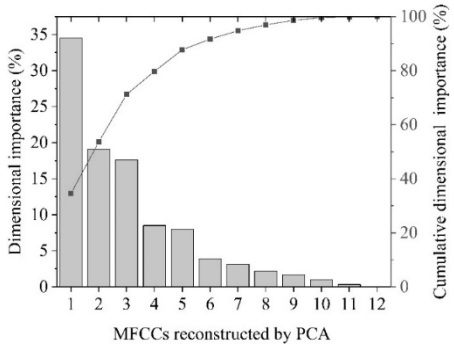

Fig. 8 Importance ranking of different reconstruction features

3.3 Feature selection

Although the two new features presented in section 3.1 and section 3.2 have been proven to be effective, it is still necessary to compare the two features with some common vibration signal features (Table 2) for an optimal feature combination. The feature that is too high related to other features is not able to bring additional useful information to recognition model, but complicate the classifier. Therefore, the maximal information coefficient is employed to exclude the redundant features. Features whose MIC are over 0.65 are considered to be strongly correlated to each other and only one of them should be retained. The MIC in the Fig. 9 indicates that the feature 2, 3, 6, 7 and 8 have a strong correlation, and only one of them should be selected as the feature combination. The subset differential parameter feature is eventually retained as the sum of its MIC is the smallest.

The redundant features can be removed by the MIC method, however, the classification effects of the remaining features still need further investigation. The features 1, 4, 5, 6, 9, 10, 11 and 12 are evaluated based on the contributions of the features to recognition rate. The evaluation method can be specifically described as follows:

(1) Calculating the recognition rate R_{all} of the classifier trained by all the features;

(2) Calculating the recognition rate $R_{feature}$ of the

Table 2 Features for comparison

Number	Feature category	Feature	Equation
1	Feature for time series data	Mean	$\text{Meant}(y)=\frac{1}{s}\sum_{1}^{s}y(n)$
2		Standard deviation	$\text{Stdt}(y)=\sqrt{\frac{\sum_1^s(y(n)-Mean(y))^2}{s-1}}$
3		Maximum	$\text{Max}(y)=max(y(n))$
4		Kurtosis	$\text{Kur}(y)=\frac{1}{s}\frac{\sum_1^s(y(n)-Mean(y))^4}{\text{Std}(y)^4}$
5		Short-time zero-crossing rate	$Zero(y)=\frac{1}{2}\sum_{n=2}^{s}\lvert sgn[y(n)]-sgn[y(n-1)]\rvert$ $sgn[x]=\begin{cases}1, & y(n)\geq 0\\ -1, & y(n)<0\end{cases}$
6		Subset differential parameter*	Details shown in section 3.1
7	Feature for frequency series	Mean	$\text{Meanf}(P)=\frac{1}{z}\sum_{1}^{z}P(k)$
8		Standard deviation	$\text{Stdf}(P)=\sqrt{\frac{\sum_1^z(P(k)-Mean(P))^2}{z-1}}$
9		Center of gravity	$\text{Graf}(P)=\frac{\sum_1^z P(k)\,k}{\sum_1^z P(k)}$
10		MFCC-PCA dimension 1*	Details shown in section 3.2
11		MFCC-PCA dimension 2*	
12		MFCC-PCA dimension 3*	

*The features with an asterisk are presented in this paper

classifier trained by the feature combination that do not contain the evaluated feature;

(3) The change C of recognition rate is obtained by the Eq. (7) and processed by Eq. (8) to acquire the importance parameter of the feature.

$$C = R_{all} - R_{feature} \tag{7}$$

$$\lambda_i = \frac{ln(C_i - 1)}{\sum_{i=1}^{k} ln(C_i - 1)} \tag{8}$$

where λ_i is the feature importance of the i-th feature and k is the number of all features.

As shown in Fig. 9, the sum of the importance parameters of the short-time zero-crossing rate feature, the

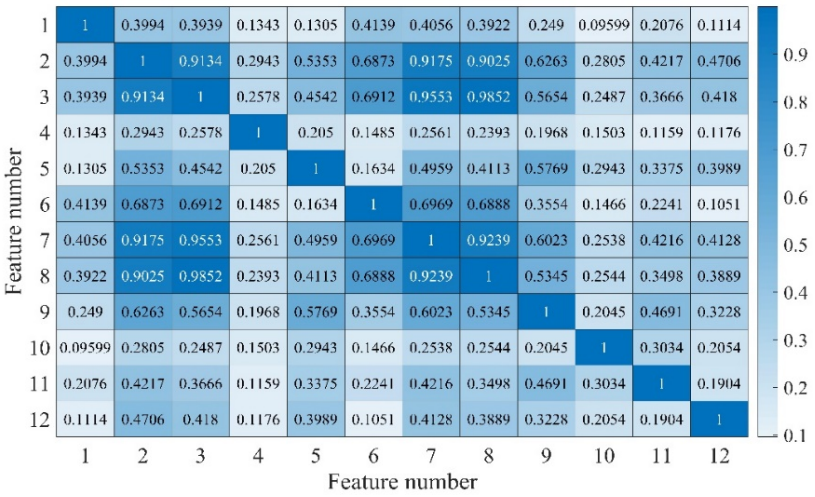

Fig. 9 MIC between features

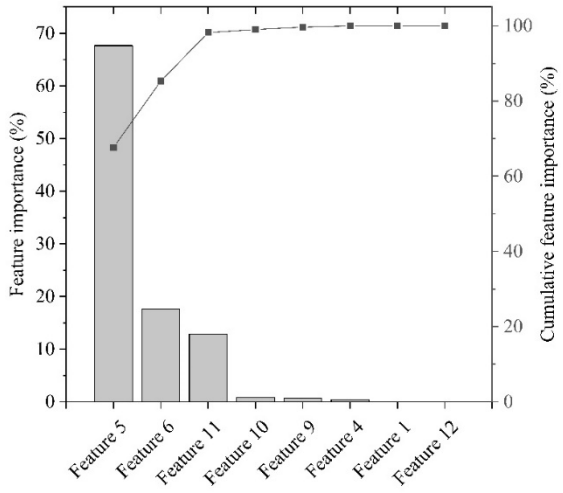

Fig. 10 Importance parameter ranking of different features

subset differential parameter and the MFCC-PCA dimension 2 feature reaches 98.18%. Therefore, these three features are selected as the feature combination of further classifier training.

4. Multi-time scale classifier training

4.1 Random forest algorithm

Table 3 Training set and testing set

Third-party interference	Range (m)	Training set/Testing set(s)	
		Traffic noise	Pedestrian noise
Road cutter	3-20	230/900	230/900
Excavator breaking hammer	5-45	70/280	70/280
No construction equipment	N/A	130/540	17490/69950

The random forest is a machine learning algorithm proposed by Leo Breiman and Adele Cutler (Breiman 2001). The classifier trained by this algorithm can identify unknown vibration signals according to the information from the training sets. A random forest classifier consists of multiple decision trees (Pradhan 2013). Every decision tree identifies unknown vibration signals, and the result of the random forest model is up to the voting results of the decision trees. The training flow of decision trees is as follows:

(1) Randomly generate A sets TS_1, TS_2, … , TS_A (A is equal to the number of the trained decision trees) by resampling based on Bootstrap method (Wu 1986) as the training sets of N decision trees.
(2) m (an integer greater than 0 and less than the total number of features) features are first selected from all the features as the splitting feature selection set of the current node, and then the node of the decision tree is split with the best-performing feature in the selection set.
(3) Each decision tree grows without pruning.

4.2 Classifier training

Based on the field tests in section 2, as presented in Table 3, there are 18220 s records for training set and 72850 s records for testing set. The time scale of the classifier has a significant effect on the recognition effect, so it is helpful in selecting and combining the classifiers of different time scales. First of all, the 300 s records of different conditions from the testing set is divided into the training samples of 0.1-10 s. The three features selected in section 3 are then calculated and combined based on the samples of different time scales. In the end, the feature combinations under different time scales are input into the random forest algorithm for the comparison of the recognition rates.

In the Table 4, the combination of 0.5 s classifier and 8 s

Table 4 Recognition rates of different time scale classifiers

Time scale 1(s)	Time scale 2(s)												
	0.1	0.2	0.5	1	2	3	4	5	6	7	8	9	10
0.1	70.9%	76.4%	78.0%	74.0%	75.1%	74.0%	75.7%	74.7%	75.6%	74.8%	79.7%	74.7%	74.9%
0.2		74.6%	79.7%	76.5%	76.7%	75.8%	77.2%	76.0%	77.1%	76.4%	81.1%	76.2%	77.1%
0.5			70.9%	76.9%	78.1%	75.3%	78.2%	76.6%	78.7%	77.4%	82.5%	76.9%	76.5%
1				62.5%	75.1%	72.0%	75.3%	74.3%	75.4%	74.4%	79.5%	74.1%	71.8%
2					73.3%	73.9%	75.8%	74.1%	75.8%	74.6%	79.8%	74.3%	75.0%
3						61.6%	73.0%	68.8%	73.6%	70.8%	77.1%	71.0%	69.8%
4							70.8%	73.0%	75.3%	74.1%	79.3%	74.4%	73.8%
5				*				66.3%	74.1%	71.8%	78.0%	71.1%	71.3%
6									73.3%	74.8%	79.0%	74.4%	76.0%
7										70.8%	78.8%	72.5%	72.9%
8											76.8%	78.3%	78.8%
9												69.1%	72.6%
10													61.3%

*The recognition rate result is symmetrical

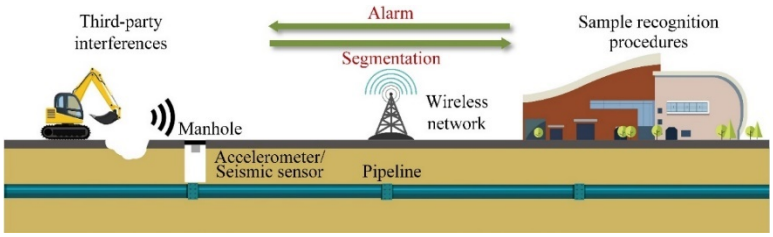

Fig. 11 Monitoring flow

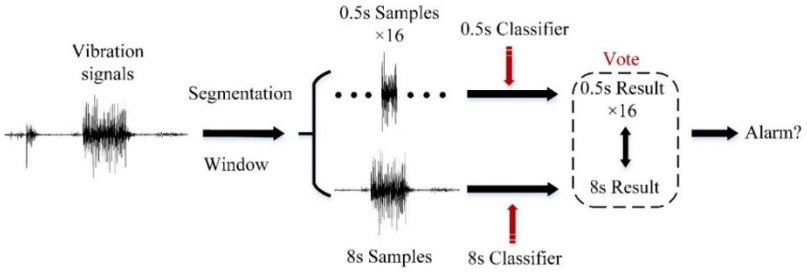

Fig. 12 Sample recognition procedure

classifier reach the highest recognition rate. The wrong results that can be corrected by 8 s classifier account for 39.86% of all errors in 0.5 s classifier, and 24.57% of mistakes in 8 s classifier are corrected by the 0.5 s classifier. The two percentages indicate that the complementation between the two classifiers can enhance the accuracy of the monitoring system. The 0.5 s and 8 s classifiers are finally trained by the training set based the conclusions of this section.

5. Monitoring flow and testing result

5.1 Monitoring flow

Based on the two classifiers trained by the samples of 0.5 s and 8 s, a flow for the pipeline third-party interference can be set up. As shown in Figs. 11 and 12, the flow is mainly followed by the steps:

(1) Vibration signals collection — recording vibration signals by accelerometers placed along the pipelines. For built pipelines, it is a superior choice to lay sensors under the manhole cover. Generally, the distance between the two adjacent sensors should be set to 50 m.

(2) Signal segmentation — obtaining samples by segmenting vibration records. The vibration signals collected by the accelerometers are segmented and windowed for 0.5 s samples and 8 s samples.

(3) Identifying 0.5 s samples and 8 s samples — for the samples of 0.5 s and 8 s, calculating their three features mentioned in section 3 and identifying them by classifier 1 and classifier 2 respectively. Obviously, one result of classifier 2 corresponds to sixteen results of classifiers 1.

(4) Voting for fusing classification results — fusing the sixteen results from classifier 1 and the one result from classifier 2 by voting, as presented in Eq. (9). The number of votes for each category is counted and the final result of the sample recognition is the category with the most votes. A result from classifier 2 is usually more valuable than a result from classifier 1 because of longer sample length. Therefore, it is obvious that the results from classifier 2 should have greater voting rights than the results from classifier 1. The parameter B_{long} is added to the Eq. (9) to adjust the voting rights of different classifiers. This parameter should be greater than 1 for the importance of classifier 2 votes, and cannot exceed the total votes of classifier 1 to avoid that the final result is completely determined by classifier 2. In this paper, the B_{long} is set to 6 according to the testing results.

$$N_{vote} = N_{short} + B_{long} N_{long} \tag{9}$$

where N_{vote} is the total number of votes obtained for a certain type of third-party interference or environmental noise; N_{short} is the number of votes from classifier 1; N_{long} is the number of votes from classifier 2.

(5) Sending alarm — sending alarm by wireless network if the recognition result is a certain kind of interference over a period of time.

5.2 Testing result

In this part, the testing set shown in Table 3 are used to address two issues of the surveillance system: the capability of the detecting threat vibration signals and the probability of sending wrong alarm under the most common urban noise condition. There are hence two radios proposed for evaluating the testing results, and recognition rate (R) that represents the detectability is defined by

$$R = T_r / T_a \tag{10}$$

Table 5 Recognition rate of the monitoring system

Third-party interference	R of different noise	
	Traffic noise	Pedestrian noise
Road cutter	91.31%	100%
Excavator breaking hammer	96.61%	96.61%
Overall	93.96%	98.31%

Table 6 False alarm rate of the monitoring system

Rate	F of different noise		Overall
	Traffic noise	Pedestrian noise	
False alarm rate	0%	0.89%	0.45%

where T_r is the number of the third-party interference samples detected by the system; T_a is the total number of third-party interference samples.

The false alarm rate (F) which corresponds to anti-noise ability can be calculated by

$$F = T_p/T_b \tag{11}$$

where T_p is the number of the environmental noise samples causing false alarm; T_b is the total number of the environmental noise samples.

It can be seen from Tables 5 and 6 that the average recognition rate and the average false alarm rate of the monitoring system are 96.14% and 0.45%, which indicates that the proposed system can effectively prevent the third-party interference around the pipeline under the pedestrian noise and the traffic noise.

6. Conclusions

Third-party interference has become the most common cause of underground pipeline accidents in recent years. Following the process of "signal collection—feature extraction and selection—multi-time scale identifying—combining results by voting", this paper proposes a multi-time scale surveillance system for prevention of third-party threats.

The working vibration of excavator breaking hammer and road cutter are collected as typical signals of third-party interference. Two kinds of noise signals induced by pedestrian and traffic are also recorded to simulate common urban application scenarios.

The three features including the classical short-time zero-crossing rate, subset differential parameter and MFCC-PCA are used to depict the differences between interference signals and noise signals. The crucial part of the surveillance system consists of the two classifiers trained by 0.5 s samples and 8 s samples respectively. Whether the system sends an alert or not is up to the voting results of the two classifiers, which contributes to enhance the accuracy of system.

In the test, the detected threats account for 96.14% of all interference events, while only 0.45% of the noise records causes false alarms. Therefore, the proposed system can effectually prevent the third-party interference and is promising in contributing to urban pipeline protection.

Acknowledgments

The authors would like to acknowledge the National Natural Science Foundation of China (Grant No. 51878509) and the State Key Laboratory of Disaster Reduction in Civil Engineering (Project: SLDRCE19-B-25) for the financial support to perform the work in this project.

References

Banu, V.C., Costea, I.M., Nemtanu, F.C. and Bădescu, I. (2017), "Intelligent video surveillance system", *Proceedings of the 23rd International Symposium for Design and Technology in Electronic Packaging*, Constanta, Romania, October.

Bock, Y., Prawirodirdjo, L. and Melbourne, T.I. (2004), "Detection of arbitrarily large dynamic ground motions with a dense high-rate GPS network", *Geophys. Res. Lett.*, **31**(6). https://doi.org/10.1029/2003GL019150

Bock, Y., Melgar, D. and Crowell, B.W. (2011), "Real-time strong-motion broadband displacements from collocated GPS and accelerometers", *Bull. Seismol. Soc. Am.*, **101**(6), 2904-2925. https://doi.org/10.1785/0120110007

Breiman, L. (2001), "Random forests", *Mach. Learn.*, **45**(1), 5-32. https://doi.org/10.1023/A:1010933404324

EGIG (2018), "10th report of the European gas pipeline incident data group", VA 17.R.0395; European Gas Pipeline Incident Data Group, Europe.

Fahmy, H.M.A. (2016), *Wireless Sensor Networks*, Springer, Singapore.

Fernández, J., Calavia, L., Baladrón, C., Aguiar, J.M., Carro, B., Sánchez-Esguevillas, A., Alonso-López, J.A. and Smilansky, Z. (2013), "An intelligent surveillance platform for large metropolitan areas with dense sensor deployment", *Sensors*, **13**(6), 7414-7442. https://doi.org/10.3390/s130607414

Ghatak, S., Bose, S. and Roy, S. (2014), "Intelligent wall mounted wireless fencing system using wireless sensor actuator network", *Proceedings of the 2014 International Conference on Computer Communication and Informatics*, Coimbatore, India, January.

Hausamann, D., Zirnig, W., Schreier, G. and Strobl, P. (2005), "Monitoring of gas pipelines-a civil UAV application", *Aircr. Eng. Aerosp. Technol.*, **77**(5), 352-360. https://doi.org/10.1108/00022660510617077

Jiang, F., Li, H., Zhang, Z. and Zhang, X. (2018), "An event recognition method for fiber distributed acoustic sensing systems based on the combination of MFCC and CNN", *Proceedings of the 2017 International Conference on Optical Instruments and Technology*: *Advanced Optical Sensors and Application*, Beijing, China, January.

Li, S., Guo, Y., Xu, Y. and Li, Z. (2019), "Real-time geometry identification of moving ships by computer vision techniques in bridge area", *Smart Struct. Syst., Int. J.*, **23**(4), 359-371. https://doi.org/10.12989/sss.2019.23.4.359

Liu, P., Chen, A.Y., Huang, Y.N., Han, J.Y., Lai, J.S., Kang, S.C., Wu, T.H., Wen, M.C. and Tsai, M.H. (2014), "A review of rotorcraft unmanned aerial vehicle (UAV) developments and applications in civil engineering", *Smart Struct. Syst., Int. J.*, **13**(6), 1065-1094. https://doi.org/10.12989/sss.2014.13.6.1065

Makhoul, N., Limongelli, M.P. and Jaoude, R.A. (2018), "Structural Health Monitoring of buried pipelines under seismic

hazard: A reivew of damage scenarios and sensing techniques", *Proceedings of the 16th European conference on Earthquake Engineering*, Thessaloniki, Greece, June.

Martínez, A.M. and Kak, A.C. (2001), "PCA versus LDA", *IEEE Transact*. *Pattern Anal*. *Mach*. *Intell*., **23**(2), 228-233. https://doi.org/10.1109/34.908974

Muhlbauer, W.K. (2004), *Pipeline risk management manual*: *ideas*, *techniques*, *and resources*, Third Edition, Elsevier, Netherlands.

Okada, Y., Kasahara, K., Hori, S., Obara, K., Sekiguchi, S., Fujiwara, H. and Yamamoto, A. (2004), "Recent progress of seismic observation networks in Japan—Hi-net, F-net, K-NET and KiK-net", *Earth Planets Space*, **56**(8), 15-28. https://doi.org/10.1186/BF03353076

Peng, F., Wu, H., Jia, X.H., Rao, Y.J., Wang, Z.N. and Peng, Z.P. (2014), "Ultra-long high-sensitivity Φ-OTDR for high spatial resolution intrusion detection of pipelines", *Optics Express*, **22**(11), 13804-13810. https://doi.org/10.1364/OE.22.013804

PHMSA (2017), "2017 Hazmat summary by mode of transportation/cause", Pipeline and Hazardous Materials Safety Administration, U.S. Department of Transportation, Washington, USA.

Pradhan, B. (2013), "A comparative study on the predictive ability of the decision tree, support vector machine and neuro-fuzzy models in landslide susceptibility mapping using GIS", *Comput*. *Geosci*., **51**, 350-365. https://doi.org/10.1016/j.cageo.2012.08.023

Reshef, D.N., Reshef, Y.A., Finucane, H.K., Grossman, S.R., McVean, G., Turnbaugh, P.J., Lander, E.S., Mitzenmacher, M. and Sabeti, P.C. (2011), "Detecting novel associations in large data sets", *Science*, **334**(6062), 1518-1524. https://doi.org/10.1126/science.1205438

Sun, J. and Wen, J. (2013), "Target location method for pipeline pre-warning system based on HHT and time difference of arrival", *Measurement*, **46**(8), 2716-2725. https://doi.org/10.1016/j.measurement.2013.04.059

Sun, Q., Feng, H., Yan, X. and Zeng, Z. (2015), "Recognition of a phase-sensitivity OTDR sensing system based on morphologic feature extraction", *Sensors*, **15**(7), 15179-15197. https://doi.org/10.3390/s150715179

Tejedor, J., Maciasguarasa, J., Martins, H.F., Piote, D., Pastorgraells, J., Martinlopez, S., Corredera, P., Gonzalezherraez, M. (2017), "A novel fiber optic based surveillance system for prevention of pipeline integrity threats", *Sensors*, **17**(2), 355. https://doi.org/10.3390/s17020355

Tejedor, J., Macias-Guarasa, J., Martins, H.F., Pastor-Graells, J., Martín-López, S., Guillén, P.C., De Pauw, G., De Smet, F., Postvoll, W., Ahlen, C.H. and González-Herráez, M. (2018), "Real field deployment of a smart fiber-optic surveillance system for pipeline integrity threat detection: Architectural issues and blind field test results", *J. Lightwave Technol*., **36**(4), 1052-1062. http://dx.doi.org/10.1109/JLT.2017.2780126

Wan, C. and Mita, A. (2009), "Pipeline monitoring using acoustic principal component analysis recognition with the Mel scale", *Smart Mater*. *Struct*., **18**(5), 055004. http://dx.doi.org/10.1088/0964-1726/18/5/055004

Wang, N., Fang, N. and Wang, L. (2019), "Intrusion recognition method based on echo state network for optical fiber perimeter security systems", *Optics Communications*, **451**, 301-306. http://dx.doi.org/10.1016/j.optcom.2019.06.058

Wu, C.F.J. (1986), "Bootstrap and other resampling methods in regression analysis", *Annals Statist*., **14**(4), 1261-1295. http://dx.doi.org/10.1214/aos/1176350142

Wu, H., Xiao, S., Li, X., Wang, Z., Xu, J. and Rao, Y. (2015), "Separation and determination of the disturbing signals in phase-sensitive optical time domain reflectometry (Φ-OTDR)", *J. Lightwave Technol*., **33**(15), 3156-3162. http://dx.doi.org/10.1109/JLT.2015.2421953

Zhang, Y. (2018), "Vibration Characteristic Analysis and Pattern Recognition of Third Party Instrusion in Buried Pipelines", M.D. Dissertation, Tongji University, Shanghai, China.

Zhang, Y. and Li, S.Z. (2018), "Pipeline incident statistics from 2010 to 2017", Department of Structural Engineering, Tongji University, Shanghai, China.

Zhang, Y.L., Zhang, Z.Q., Xiao, G., Wang, R.D. and He, X. (2015), "Perimeter intrusion detection based on intelligent video analysis", *Proceedings of the 15th International Conference on Control*, *Automation and Systems* (*ICCAS*), Busan, South Korea, October.

Zheng, F., Zhang, G. and Song, Z. (2001), "Comparison of different implementations of MFCC", *J. Comput*. *Sci*. *Technol*., **16**(6), 582-589. http://dx.doi.org/10.1007/BF02943243

Zhu, Y., Lei, Z., Zheng, W., Ma, H., Xia, R. and Song, D. (2019), "Research on substation perimeter isolation based on phased array radar and multi-video fusion technology", *Journal of Physics*: *Conference Series*, **1187**(2), 22-54. http://dx.doi.org/10.1088/1742-6596/1187/2/022054

HJ